Behaviour of Soft Clay Deposit Subjected to Long-term Cyclic Shear Stresses

Masayuki HYODO*, Kazuya YASUHARA**, Hidekazu MURATA*
and Kazutoshi HIRAO**

(Received July 14, 1988)

Abstract

The purpose of the present paper is to depict the clay behaviour under long-term cyclic shear conditions. The empirical relations of time-dependent shear deformation and cyclically induced pore pressure were formulated through the undrained cyclic triaxial test on plastic clay. An analytical model was presented by combination of the equation of induced pore pressure with the Terzaghi's type of consolidation theory. The model successfully explained the behaviour of generation and dissipation of pore pressure and volumetric change in clay during cyclic loading. It was suggested that the proposed model should be a clue to to predict the deformation, settlement and stability of soft clay under long-term cyclic loading with inclusion of drainage.

1. Introduction

When the soft clays are subjected to such long-term cyclic loading as traffic loads, the grounds might induce harmful settlements. There have been several cases that embankments for highways constructed on clays suffered from abnormal settlements after beginning of travelling the motor vehicles (Yamanouchi et al[5),6)], Yasuhara et al[7)], Hyodo et al [2)]). The soil elements subjected to long-term cyclic loadings are supposed to be in partial drained condition with generation and dissipation of pore pressure. The main scope of the present study is to investigate the clay behaviour in drained and undrained cyclic loading through triaxial tests on a highly plastic marine clay. At the same time, an analytical model is pursued for predicting the behaviour of deformation and pore pressure of clay deposits under long-term cyclic shear conditions.

2. Mechanism of Clay Deformation under Long-term Cyclic Loading and Test's Procedure

Clay deformation under long-term cyclic loading with inclusion of drainage may constitute :

1) shear deformation under undrained cyclic loading,

2) volume change due to dissipation of cyclically induced pore pressure.

The schematic diagram for explaining this behaviour is shwn in Fig. 1. The total

---

*Department of Civil Engineering (Kensetu)
**Nishinippon Institute of Technology

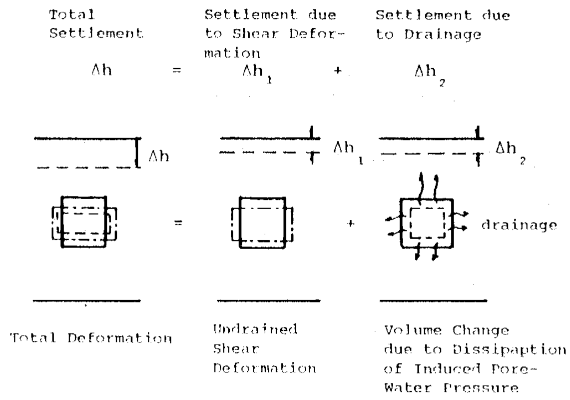

Fig. 1 Schematic diagram for explaining the settlement of ground due to long-term cyclic loading.

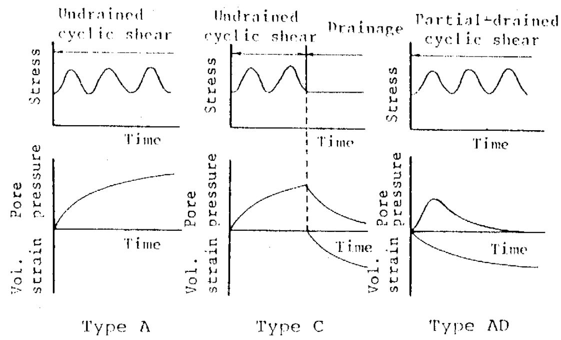

Fig. 2 Three types of cyclic triaxial tests performed in this study.

deformation is evaluated by the combination of these two factors. In order to investigate these factors individually, the following three types of cyclic triaxial tests as shown in Fig. 2 were carried out.

1) Undrained cyclic triaxial tests (type-A).

Results from this type of tests were used to estimate the residual shear strain and pore pressure.

2) Undraind cyclic triaxial tests followed by drainage (type-C).

In these tests, drainage is permitted after a certain number of load cycles is applied to the specimen and the coefficients of volume compressibility and permeability were determined from measurement of volumetric strain due to dissipation of cyclically induced pore pressure.

3) Drained cyclic triaxial test (type-AD).

The cyclic load is applied to a specimen under drained conditions by opening the drainage system. Throughout the cylindrical specimen (3.5cm in diameter and 8.75cm in height) in triaxial cell, distribution of pore pressure is not homogeneous during drained cycling because of low permeability of clay. In this sense, this type of cyclic test can

Table 1 Conditions of cyclic triaxial compression tests on Ariake clay.

Test No.	σ_c (kPa)	$\Delta\sigma_a$ (kPa)	N (cycle)	w_i (%)	e_c
A－1	200	40	3600	95.6	2.021
A－2	200	80	3600	83.3	1.982
A－3	200	100	3600	90.6	1.953
A－4	200	120	3600	93.8	1.960
A－5	200	140	3600	90.5	1.871
A－7	200	100	172800	92.5	1.934
A－10	200	120	172800	93.2	1.893
A－15	100	36	3600	93.8	2.086
A－16	100	64	3600	94.5	2.071
A－17	100	86	3600	93.3	2.084
A－18	300	76	3600	94.1	1.822
A－19	300	137	3600	95.6	1.861
C－1	200	100	3600	90.9	1.895
C－2	200	120	172800	91.7	1.896
C－3	200	140	3600	92.7	1.895
C－4	200	80	172800	91.6	1.915
C－5	200	80	3600	92.2	1.915
C－6	200	80	17280	91.4	1.850
C－7	200	80	360	83.3	1.952
C－10	200	80	5000	81.8	1.972
C－11	200	80	87000	92.4	1.869
C－12	200	80	3600	91.2	1.894
AD－1	100	40	3600	94.3	2.013
AD－2	100	60	3600	93.1	2.000
AD－3	100	80	3600	93.0	2.039
AD－4	200	80	3600	93.1	1.895
AD－5	200	120	3600	93.5	1.850
AD－6	200	160	3600	82.5	1.861
AD－8	300	120	3600	92.1	1.708
AD－9	300	130	3600	92.7	1.688
AD－10	300	240	3600	93.2	1.741

be classified as a partial-drained shear test.

Reconstituted highly plastic clay called" Ariake clay" was used in these tests. Index properties and some mechanical parameters are :
$G_s=2.65$, $w_L=123\%$, $I_p=69$, $C_c=0.700$, $C_s=0.163$ and $\phi'=39^\circ$. The clay cylinder was trimmed as a specimen for every triaxial test from the clay block which was fully preconsolidated under 59kPa of vertical pressure in the large consolidation vessel. The water content was 90 to 95% on the average.

Pore pressure was measured through the porous stone with 3mm in diameter buried in the center of lower pedestal. Drainage was done from the side wall around the lower pedestal through the drain paper surrounding the specimen. The conditions of cyclic triaxial tests were summarized in Table 1. The cylindrical specimens for the triaxial tests were isotropically preconsolidated for 24 hrs under the confining pressures of 100, 200 and 300kPa. Then, cyclic loading, one-way loading in compression side, starts after isotropic consolidation. The number of load cycles was 3600 for most of tests to 172800 as the maximum.

3. Formulation of Pore Pressure and Residual Shear Strain in Undrained Cyclic Triaxial Test

The pore pressure and axial strain were measured in undrained cyclic triaxial tests. They depended on the confining pressure and the cyclic load intensity and the number of load cycles. It is, therefore, assumed that both the pore pressure ratio and the axial strain can be formulated as a function of the stress ratio and the number of load cycles. Regression analyses for these formulations were performed and the following relations were obtained.

$$u_g/\sigma_c = 0.064(\Delta\sigma_a/\sigma_c)^{1.418}\ (log10N)^{1.535} \tag{1}$$

$$\varepsilon_a = 0.096(\Delta\sigma_a/\sigma_c)^{1.745}(log10N)^{1.763} \tag{2}$$

Fig. 3 and 4 show the variations of residual strain and pore pressure ratio with the number of load cycles, respectively. All of the observed values are compared with the regression curves given by eqs. (1) and (2). The coefficients of correlation resulted from the regression analyses are about 0.93~0.94 which may be considered to be a fairly high value. In both kinds of figures, the results are presented classifying them by the confining pressure. It is recognized that the calculated values by the empirical equations are in fairly good agreement with the observed values, especially in the pore pressure versus the number of load cycles relations. Judging from this fact, it can be said that eqs. (1) and (2) are available for describing the behaviour of normally consolidated clay under long-term cyclic loading.

When we are trying to apply the result obtained by triaxial test to the practical problem, it is often necessary to exchange the quantity of axisymmetric condition to that of plane strain. Now, we are going to correspond each maximum shear stress on the plane bisecting the angle between the two principal stresses. Then eqs. (1) and (2) are rewritten into the function of maximum shear stress $\Delta\tau_{max}$ and number of load cycles. Further, the axial strain ε_a is converted into the maximum shear strian γ_{max}, and cyclic axial stress $\Delta\sigma_a$ into the maximum shear stress as shown in the following equations :

$$\Delta\sigma_a = 2\Delta\tau_{max} \tag{3}$$

$$\varepsilon_a = 4/3\gamma_{max} \tag{4}$$

Substituting above equations into eqs. (1) and(2), the following equations are obtained.

$$u_g/\sigma_c = 0.171(\Delta\tau_{max}/\sigma_c)^{1.418}(log10N)^{1.535} \tag{5}$$

$$\gamma_{max} = 0.241(\Delta\tau_{max}/\sigma_c)^{1.745}(log10N)^{1.763} \tag{6}$$

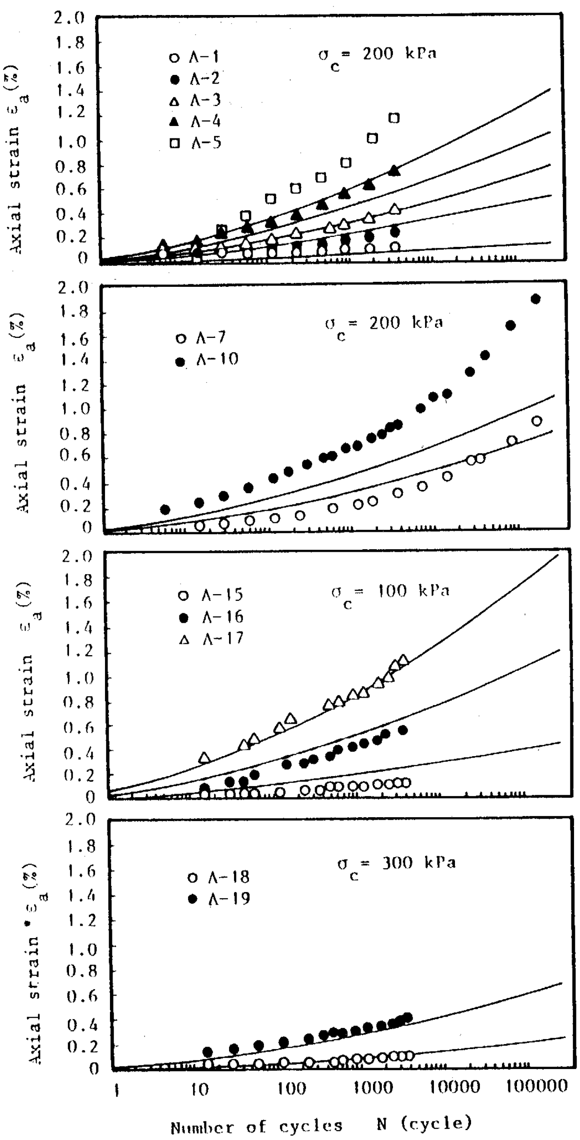

Fig. 3 Variation of residual axial strain with number of load cycles.

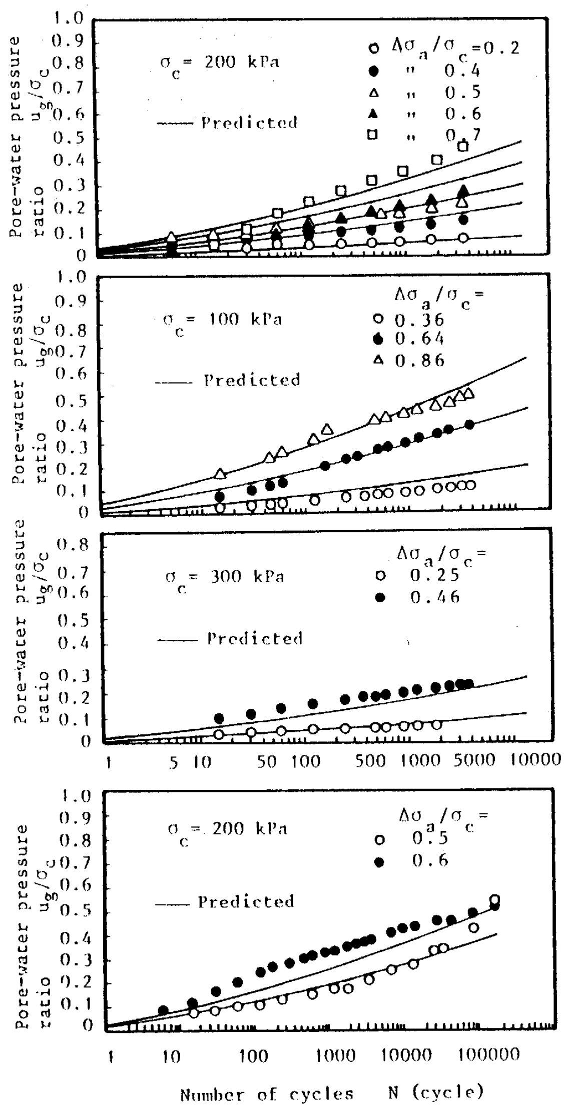

Fig. 4 Variation of pore pressure with number of load cycles.

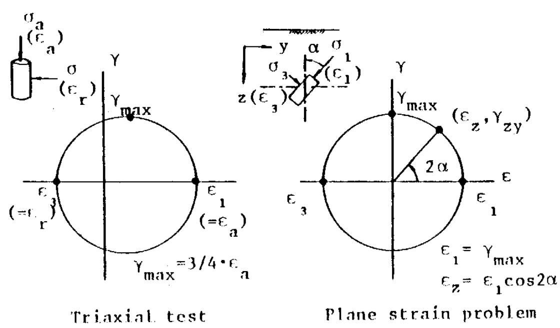

Fig. 5 Correlation of strain states between axisymmetric and plane strain condition in undrained cyclic loading.

The correlation of strain state between plane strain and axisymmetrical condition in undrained cyclic triaxial test is presented by the Mohr's strain circles as shown in Fig. 5. In the undrained condition, it is satisfied to keep the following relation: $\varepsilon_1+\varepsilon_3=0$, in the plane strain, and $\varepsilon_1+2\varepsilon_3=0$, in the axisymmetrical condition, respectively. If the maximum shear stresses in the plane strain and triaxial test can be corresponded each other, the maximum shear strain is calculated using eq. (6) also in the plane strain problem. Then the major principal strain is obtained because there is a relation of $\varepsilon_1=\gamma_{max}$ in the Mohr's circle. Further, an arbitrary component of strain can be calculated if the angle of objective plane from the principal plane would be known. Thus, taking the angle between the vertical direction and the major principal axis to be α, the vertical strain is calculated as :

$$\varepsilon_z=\varepsilon_1\cos 2\alpha \tag{7}$$

4. Prediction of Behaviour in Drained Cyclic Triaxial Test

4.1 Concept of Partial-Drained Condition

As mentioned above, the drained cyclic triaxial test is assumed to be a partial-drained shear test. According to the research work on the effect of partial drainage of sand, subsequent undrained shear is affected by the process of partial drainage in case where a significant amount of pore pressure is dissipated during each cycle (O-hara et al[3], Umehara et al[4]). In comparison with sand, the effect of dissipation on clay behaviour is not significant in each cycle but it would be accumulated during long-term cyclic loading, while it is regarded as undrained in case of short-term cyclic loading condition such as at earthquake.

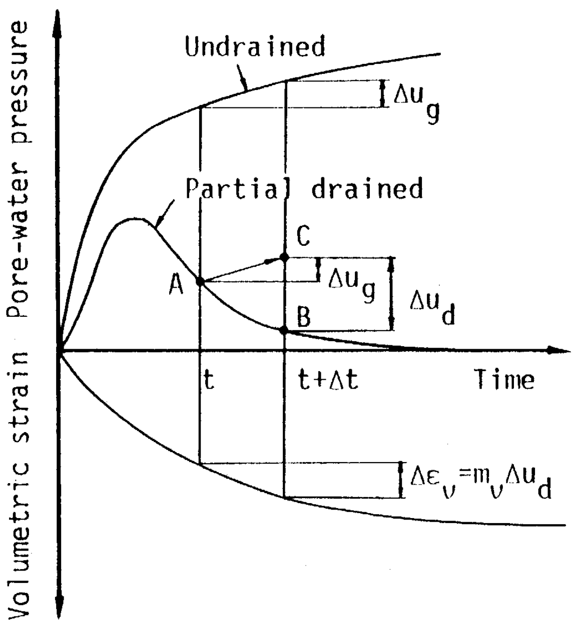

Fig. 6 Schematic diagram for pore pressure and volumetric strain in partial-drained cyclic shear condition.

4.2 Analytical Model

The model for presenting the partial-drained behaviour of clay was developed as shown in Fig. 6. In partial-drained condition, the time dependent pore pressure traces the curve with a peak, the middle curve in Fig. 6, and volumetric strain traces the monotonically increasing curve like the figure. In the analytical model, it is assumed that the incremental pore pressure produced by undrained cyclic loading during a time interval Δt should be superimposed on the above mentioned pore pressure. Then, a part of this superimposed pore pressure dissipates as a soil element follows A→C→B path as shown in Fig. 6. The volumetric strain $\Delta\varepsilon_v$, during path C→B under the partial -drained conditon is written as

$$\Delta\varepsilon_v = m_v \Delta u_d \qquad (8)$$

The following equation which was originally introduced by Booker et al[1] was employed as the governing equation for the partial-drained behaviour of clay.

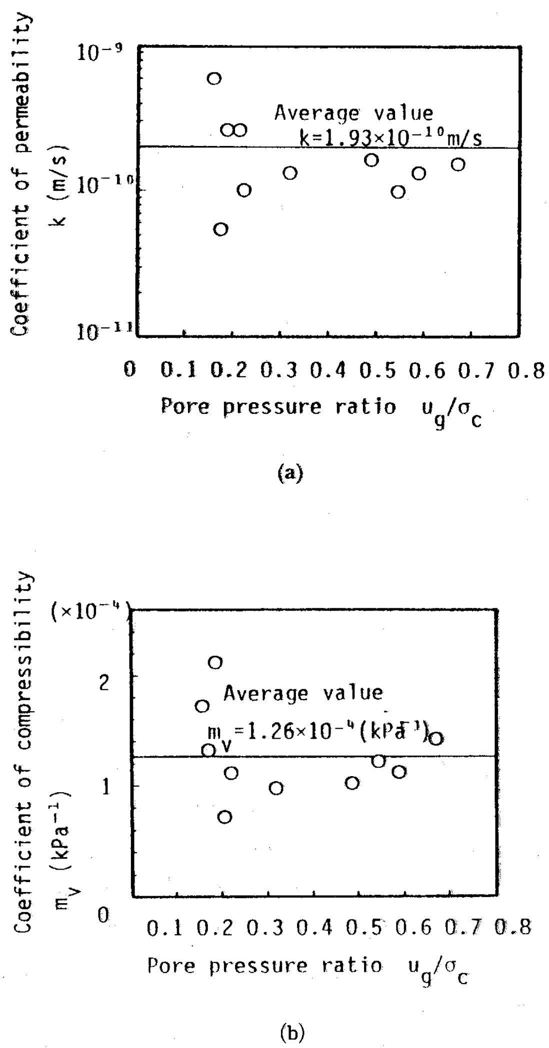

Fig. 7 Coefficients obtained by post-cyclic recompression tests : (a) Coefficient of permeability, (b) Coefficient of volume compressibility

$$\{\nabla\}^T[K]\left\{\nabla\frac{u}{\gamma_w}\right\}=m_v\left\{\frac{\partial u}{\partial t}-\frac{\partial u_g}{\partial t}\right\} \tag{9}$$

in which [K] : permeability matrix, u_g : cyclically induced pore pressure.

The parameters contained in the governing equation are the coefficients of permeability and volume compressibility. Those were determined by the results from post-cyclic recompression tests (so called type-C test). The observed values of those coefficients are illustrated in Fig. 7(a), (b). Although the number of data is limitted and plots are somewhat scattering, it can be said that those two coefficients are kept constant independent of the cyclically induced pore pressure ratio.

4.3 Analysis

Numerical analyses using the finite element method were conducted for the clay cylinder in triaxial tests under partial-drained conditions. A sketch of specimen and its fininte element model are presented in Fig. 8. The boundary condition which is to be zero pore pressure is given in the side boundary of specimen. Since only the radial flow is permitted in this case, the finite element model can be replaced by the simpler one which is shown in Fig. 8 (c).

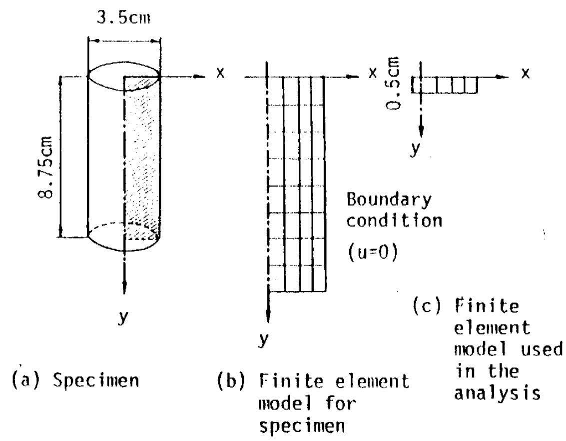

Fig. 8 Finite element model for specimen in cyclic triaxial compression test.

Fig. 9 illustrates the computed result of distribution of pore pressure buildup and dissipation in a specimen under drained cyclic loading. The result in Fig. 9 points out that the effect of drainage gradually propagates from surface to inside of a specimen while the pore pressure rises up homogeneously. Thereafter, when the peak pore pressure is attained at the center of specimen, pore pressure distribution is of the triangular shape and then pore pressure dissipates keeping the same shape of distribution until the end of drainage.

Fig. 10 shows the variations of pore pressure and volumetric strain with time in drained cyclic loading. In pore pressure, the analytical results are shown by a solid line which shows almost average line of the observed results regardless of confining pressure. However, the tendencies of analytical and observed results correspond well

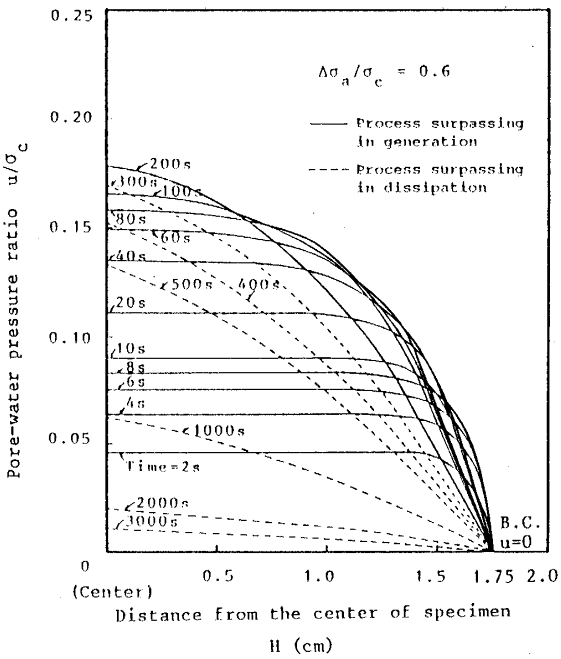

Fig. 9 Distribution of pore pressure in specimen under partial -drained condition.

each other, especially in the point of peak and the dissipation process. On the other hand, it is seen that the analytical results of volumetric strain fit fairly well with the observed plots in each confining pressure.

Fig. 11 shows the time dependent residual axial strain of drained cyclic triaxial test. The solid lines were obtained from the proposed analysis by combining the undrained axial strain and one third of volumetric strain induced by drainage of pore pressure. In the figure, the undrained axial strain is shown by a dashed line. Comparing these predicted results with the experimental ones, fairly good correspondenses are observed. Consequently it is concluded from these comparison that the proposed model is appropriate for analysis of the behaviour of clay under long-term cyclic loading.

5. Conclusions

An analytical model was proposed for evaluating the deformation of clay due to undrained shear and partial drainage of pore pressure under long-term cyclic loading. Undrained shear strain and pore pressure were detected as exponential functions. The volume change in partial-drained cyclic shear was given by combination of the consolidation equation with the formulated pore pressure. Then finite element analysis was carried out on clay specimen of drained cyclic triaxial test. Analyzed pore pressure, volumetric strain and axial strain are in good correspondence with test results.

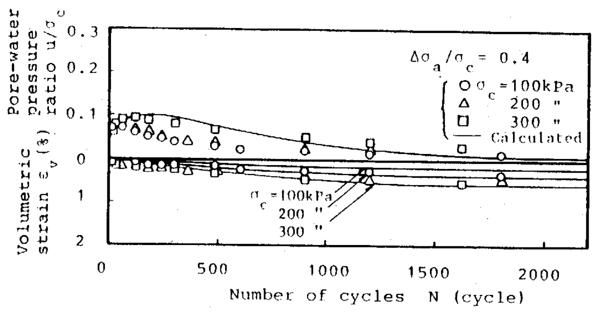

(a)

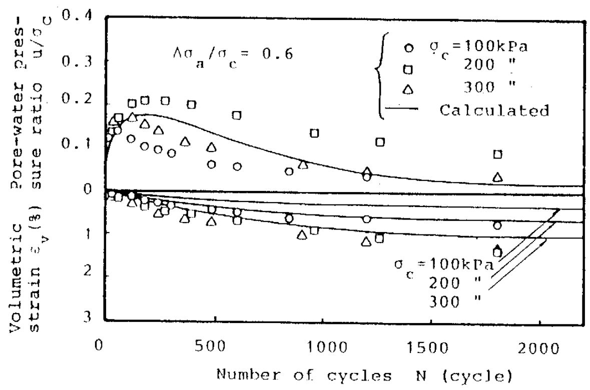

(b)

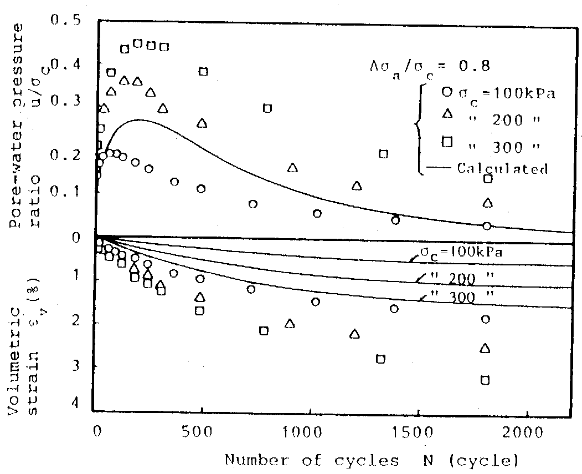

(c)

Fig. 10 Calculated and observed pore pressure and volumetric strain under partial−drained cyclic shear condition : (a) $\Delta\sigma_a/\sigma_c=0.4$, (b) $\Delta\sigma_a/\sigma_c=0.6$, (c) $\Delta\sigma_a/\sigma_c=0.8$

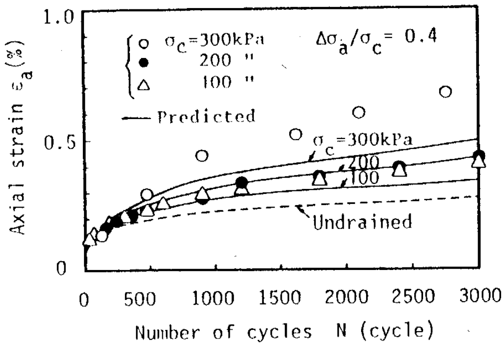

Fig. 11 Calculated and observed residual axial strain in partial-drained cyclic triaxial test.

Acknowledgement

The authors would like to express their hearty thanks to Mr. N. Yasuku of Ymaguchi University for his kind suggestions and helps.

References

1) Booker, J. R., Rahman, M. S. and Seed, H. B. "GADFLEA-A computer program for the analysis of pore pressure generation and dissipation during cyclic or earthquake loading", Report No. EERC, 76-24, Univ. Calif. (1976).
2) Hyodo, M., Yasuhara, K. and Murata, H. "Traffic induced pore pressure and deformation of soft clay deposit beneath embankment", Proc. Int. Symp. Geotech. Eng. of Soft Soils, 231-238 (1987).
3) O-hara, S., Kotsubo,S. and Yamamoto, T. "Pore pressure developed in saturated sand subjected to cyclic shear stress under partial-drainage conditions" , Soils and Foundations, **25**, [2], 45-56, (1985).
4) Umehara, Y., Zen, K. and Hamada, K. "Evaluation of soil liquefaction potentials in partially drained conditions", Soils and Foundations, **25**, [2], 57-72, (1985).
5) Yamanouchi, T. and Yasuhara, K. "Settlement of clay subgrades of low bank roads after opening to traffic", Proc. 2nd Australia-New Zealand Conf. on Geomechanics, 115-119, (1975).
6) Ymanouchi, T. and Yasuhara, K. "Deformation of saturated soft clay under repeated loading", Proc. Int. Symp. on Soft clay, 165-178 (1977).
7) Yasuhara, K., Hirao, K. and Aoto, H. "A simplified strain time relation for soils subjected to repeated loading", Int. Symp. on Soils under Cyclic and Transient Loading, 791-800, (1980).